



## Transcription factor FOXP4 inversely governs tumor suppressor genes and contributes to thyroid cancer progression

Tian Zhou<sup>a,b,1</sup>, Ning Ma<sup>a,e,1</sup>, Yong-lin Zhang<sup>b</sup>, Xing-hong Chen<sup>d</sup>, Xue Luo<sup>c</sup>,  
Mai Zhang<sup>a</sup>, Qing-jun Gao<sup>c</sup>, Dai-wei Zhao<sup>a,d,\*</sup>

<sup>a</sup> School of Clinical Medicine, Guizhou Medical University, Guiyang, 550001, Guizhou, China

<sup>b</sup> Department of Breast Surgery, Affiliated Hospital of Guizhou Medical University, Guiyang, 550004, Guizhou, China

<sup>c</sup> Department of Thyroid Surgery, Affiliated Hospital of Guizhou Medical University, Guiyang, 550004, Guizhou, China

<sup>d</sup> Department of Breast and Thyroid Surgery, Guiqian International General Hospital, Guiyang, Guizhou, China

<sup>e</sup> Department of Vascular and Thyroid Surgery, Guizhou Provincial People's Hospital, Guiyang, Guizhou, China

### ARTICLE INFO

#### Keywords:

EMT  
FBXW7  
FOXP4  
Thyroid cancer  
Tumor transplant

### ABSTRACT

**Objective:** In recent decades, thyroid cancer (TC) has exhibited a rising incidence pattern. Elevated levels of the transcription factor FOXP4 have been strongly linked to the progression of diverse tumors; nevertheless, its specific role in thyroid cancer remains underexplored. The primary objective of this study was to elucidate the functions of FOXP4 and its associated target gene, FBXW7, in the context of thyroid cancer.

**Methods:** FOXP4 and FBXW7 expression levels in TC tissues and cell lines were assessed through immunohistochemistry and RT-qPCR analyses. The functional aspects of FOXP4, including its effects on cell proliferation, migration capabilities, cell cycle regulation, and epithelial-mesenchymal transition (EMT), were investigated. Furthermore, the interaction between FOXP4 and FBXW7 was confirmed using chromatin immunoprecipitation (ChIP) assays. The impact of FBXW7 on FOXP4-mediated cellular phenotypes was subsequently examined. Additionally, the in vivo role of FOXP4 and FBXW7 in tumor growth was elucidated through the establishment of a murine tumor model.

**Results:** Elevated levels of FOXP4 were observed in papillary carcinoma tissues, and patients exhibiting high FBXW7 levels showed a more favorable prognosis. KTC-1 cells displayed a concomitant increase in FOXP4 expression and decrease in FBXW7 expression. FOXP4 overexpression in these cells enhanced cell proliferation, migration capabilities, and EMT. The interaction between the FOXP4 protein and the FBXW7 promoter was confirmed, and the effects of FOXP4 were mitigated upon overexpression of FBXW7. Furthermore, knockdown of FOXP4 led to decelerated growth of transplanted tumors and increased FBXW7 levels within the tumors.

**Conclusion:** The findings of the current study underscore the regulatory role of FOXP4 in the transcription of FBXW7 and establish a clear link between aberrations in FBXW7 expression and the manifestation of malignant phenotypes in highly aggressive TC cells.

\* Corresponding author. School of Clinical Medicine, Guizhou Medical University, Guiyang, 550001, Guizhou, China.

E-mail address: [zzhaodaiwei@126.com](mailto:zzhaodaiwei@126.com) (D.-w. Zhao).

<sup>1</sup> These authors contributed equally to this article.

<https://doi.org/10.1016/j.heliyon.2023.e23875>

Received 28 April 2023; Received in revised form 30 November 2023; Accepted 14 December 2023

Available online 7 January 2024

2405-8440/© 2024 The Authors. Published by Elsevier Ltd. This is an open access article under the CC BY-NC-ND license (<http://creativecommons.org/licenses/by-nc-nd/4.0/>).

## 1. Introduction

Thyroid cancer (TC) represents a prevalent malignant tumor within the endocrine system. With the advent of advanced high-resolution imaging techniques, particularly ultrasonography [1], and fine-needle aspiration biopsy enabling the detection of microscopic nodules [2], even thyroid tumors measuring less than 1 cm in diameter can be identified [3]. Consequently, there has been a notable increase in cancer incidence over the past two decades [4]. Data from the 2020 China Cancer Report revealed that 200,700 patients received a TC diagnosis in 2020, constituting 5.11% of all new cancer cases [5]. The age-standardized incidence rate of TC per 100,000 people was 12.05, a figure notably surpassing the global average of 10.44. TC is categorized into three distinct pathological subtypes: follicular cell-derived differentiated TC, anaplastic TC, and medullary TC [6]. Approximately 90% of all TC cases belong to the differentiated types. Among these, papillary TC stands out as the most prevalent subtype and boasts the most favorable prognosis [7], with long-term survival rates reaching close to 95%. Other examples of differentiated TC include follicular, Hürthle cell [8], and poorly differentiated carcinomas. Despite their differentiation, these types are malignant and exhibit a strong tendency for distant metastasis [9].

Surgery, radioactive <sup>131</sup>I treatment [10], and endocrine suppression are the predominant treatment approaches for TC at present [11]. Surgical resection is usually the first choice for differentiated and medullary types. Although the extent of removal of tiny tumors has been controversial [12], clinicians advocate total thyroidectomy with or without neck dissection for most differentiated or medullary TC > 1 cm in size and with a clear preoperative diagnosis [13,14]. Notably, targeted medicines like sorafenib and lenvatinib have recently been approved as therapeutic options, representing a new therapy modality [15]. This demonstrates the value of target mining in fostering new approaches to treating TC.

Forkhead box P4 (FOXP4) belongs to the P subfamily of the FOX transcription factor family and is situated on chromosome 6 [16]. The FOXP4 gene comprises leucine zipper and zinc finger domains, along with a highly conserved forkhead DNA-binding domain [17]. FOXP4 plays a pivotal role in regulating developmental programs in heart and lung tissues; its deficiency has been linked to early embryonic mortality [18]. Moreover, elevated levels of the protein encoded by FOXP4 have been linked to the progression of different types of tumors. Notably, abnormal expression of FOXP4 has been observed in breast malignancies [19], liver cancer [20], and oral squamous cell carcinoma [21]. Nonetheless, the precise functional role of FOXP4 in TC, along with the underlying mechanistic reactions, remains unexplored.

The FBXW7 gene encodes a protein with significant functions in the regulation of cellular proliferation, differentiation, and apoptosis. Mutations in FBXW7 have been associated with various cancers, including TC. The results of our study show that FOXP4 regulates FBXW7 expression by binding to its promoter. In TC cells, we propose that FOXP4 acts as a transcription factor, regulating the expression of FBXW7. Consequently, FBXW7 is considered a target of FOXP4 in TC. In this study, we employed bioinformatics analysis to predict target gene of FOXP4 and explored the roles of the FOXP4 regulatory axis in TC. The primary objective of this study is to delineate the functional roles of FOXP4 and its target gene, F-box and WD repeat domain containing 7 (FBXW7), with the aim of providing innovative targeted therapies for the treatment of TC.

## 2. Materials and methods

### 2.1. Sample collection

The Ethics Committee of the Hospital approved the current study (approval no. 2200250). All procedures were carried out in conformity with the 1964 Declaration of Helsinki. Patients diagnosed with papillary thyroid carcinoma by pathological examination at our department were enrolled, and those with other thyroid and immune system diseases were excluded. The participants were informed of the study and signed an informed consent form. TC and adjacent tissues were collected from a total of 62 patients.

### 2.2. Immunohistochemical (IHC)

Thyroid tissue sections embedded in paraffin were cut into 4 μm slices, followed by deparaffinization in xylene and rehydration using graded alcohols. Antigen retrieval was performed using an antigen unmasking solution (10 mM citrate buffer, pH 6.0) with microwave heating at 100 °C to facilitate antigen retrieval. Subsequently, any remaining endogenous peroxidase activity was neutralized using a 3% hydrogen peroxide solution. The tissue sections were incubated overnight at 4 °C with primary antibodies specific to FOXP4 (catalog number: 16772-1-AP, company: Proteintech, America). Following this, the sections were blocked with serum and exposed to appropriate secondary antibodies (catalog number: PMK-014-090MPMK-014-090S, Company: BIOPRIMACY, America). Protein visualization was achieved using a standard diaminobenzidine protocol, resulting in a brown pigment reaction. Subsequently, the slides were briefly counterstained with hematoxylin and examined under a Leica microscope to identify positive immunostaining.

### 2.3. Cell lines and transfection

Thyroid follicular epithelial cell lines, namely Nthy-ori 3-1, TC TPC-1, KTC-1, and ACT-1, were procured from the American Type Culture Collection (as listed in Table S1). These cells were cultured in DMEM (Dulbecco's Modified Eagle Medium) (Biosharp, Anhui, China) supplemented with 10% FBS (Fetal Bovine Serum) from Thermo Fisher, and maintained at a temperature of 37 °C in an atmosphere of 5% carbon dioxide.

KTC-1 cells were subjected to transfection with two distinct types of short hairpin RNA (shRNA) specifically designed to target FOXP4. A scrambled shRNA was utilized as a negative control (NC) in the experiments. Additionally, pcDNA3.1 vectors containing FOXP4 were employed to facilitate the overexpression of FOXP4. Empty vectors were used as the negative control in this context. The shRNAs and vectors were supplied by Shanghai GenePharma. Transfection of these recombinants into KTC-1 cells was carried out using Lipofectamine® 2000 (Invitrogen) following standard protocols. After transfection at 37 °C for 6 h, the culture medium was replaced with fresh, intact culture medium. The cells were then incubated at 37 °C for an additional 48 h to assess transfection efficiency. Subsequent experiments were conducted using these transfected cells.

#### 2.4. Animals and preparation of tumor transplants

The experimental procedures were approved by the Animal Ethics Committee of our hospital. Ten male Balb/c nude mice (age, 4–6 weeks; 16–18 g) were housed in temperature-controlled cages with 12 h light/dark cycle, and food and water were supplied without restriction.

The stable expression of pEGP-shRNA-FOXP4 was achieved, incorporating the green fluorescent protein (GFP)-encoding gene. Transfected KTC-1 cells (106) were suspended in a volume of 0.2 ml and injected into mice using a syringe. At three-day intervals, the mice were weighed, and the tumor size was measured, with accompanying photographs taken. On the 27th day, the mice were euthanized using a sodium pentobarbital overdose (100 mg/kg, i.p.), and the tumor tissue was harvested for subsequent assays.

Details: Prior to the experiment, all measurement tools were meticulously calibrated to ensure precision and accuracy. Accurate measuring instruments, including digital vernier calipers where applicable, were utilized. In cases where inaccuracies were identified, necessary adjustments were made, or the tools were replaced with new ones to maintain the precision of measurements. Standardized methods for tumor measurement were employed in this study. Prior to the experiment, precise methods and operational protocols were established for measuring tumors. Specialized operating procedures and standard guidelines were developed to ensure uniformity and consistency across experiments. Maintaining consistent operating methods across different experiments was essential to guarantee the accuracy and repeatability of measurement results. A suitable and consistent measurement time point was carefully chosen, and the alterations in tumor size corresponding to this specific time point were thoroughly analyzed. To prevent measurement errors, the identical measurement time point was employed for all experimental animals. Additionally, the precise location of the tumor was marked to ensure accurate and consistent measurements. Before conducting measurements, the location of the tumor was distinctly marked on the surface of the mouse's body to prevent repetitive and inaccurate measurements. Rigorous adherence to standardized measurement procedures was maintained. Throughout the measurement process, precautions were taken to avoid actions that could potentially lead to measurement errors, such as accidental contact with the mice, collisions, or sudden movements with hands.

#### 2.5. Reverse transcription-quantitative PCR (RT-qPCR)

Total RNA from the sample cells was extracted using total RNA isolation reagent (Biosharp) and then reverse-transcribed into cDNA using the Hifair® II 1st Strand cDNA Synthesis Kit (YEASEN, Shanghai). Subsequently, qPCR analysis was performed using Hieff® qPCR SYBR Green Master Mix (YEASEN). The following conditions were applied: an initial denaturation step at 95 °C for 5 min, followed by 40 cycles at 95 °C for 10 s and 60 °C for 30 s. The comparative Ct method was utilized to assess relative gene expressions, with normalization against  $\beta$ -actin (as indicated in [Table S2](#)).

#### 2.6. Cell counting kit-8 (CCK-8) assay

Initially, KTC-1 cells were seeded in a 96-well plate at a density of  $3 \times 10^4$  cells per well. Subsequently, the cells were treated with CCK-8 solution (Dojindo) at 37 °C for 2 h. The absorbance of the solution was then measured at 450 nm using a Thermo Fisher microplate reader.

#### 2.7. Colony formation assay

KTC-1 cells were seeded in a 24-well plate at a density of 500 cells per well. After 7 days of incubation, the supernatant was removed, and the cells were washed with PBS. Subsequently, the cells were fixed in 4% paraformaldehyde (Sigma) for 20 min and stained with crystal violet (Beyotime) for 10 min at room temperature. A colony was characterized as a cluster comprising more than 50 cells.

#### 2.8. Transwell assay

Cell migration capabilities were assessed using a Transwell chamber (Corning). The lower chamber was filled with DMEM containing 20% FBS. KTC-1 cells were subsequently fixed with 4% paraformaldehyde and stained with crystal violet. After a 48-h incubation period, the results were observed and recorded using a Leica microscope.

#### 2.9. Flow cytometry

The collected KTC-1 cells were washed with PBS and subsequently fixed overnight—cell pellets were fixed in pre-chilled 75%

ethanol (Zhanwang, Wuxi, China) at 4 °C overnight. After the centrifugation, cells were rinsed in ice-cold PBS. Propidium iodide solution (Beyotime) was added to cells followed by incubation at 37 °C for 30 min in the dark. Subsequently, 500 µl of cell suspension was used for detection using a flow cytometer (BD FACS AriaTMIII, USA).

2.10. Western blotting

Proteins were extracted from tissue samples or cells using RIPA lysis buffer (Biosharp). Subsequently, these proteins (25 µg) were separated on a 10% polyacrylamide gel and then transferred to PVDF membranes (Millipore). The PVDF membrane was co-incubated in TBS Tween-20 buffer (Amresco) containing 5% BSA (BioFROXX) for 1 h. Subsequently, the membrane was probed with primary antibodies at 4 °C and then with HRP-conjugated goat anti-rabbit secondary antibody for 1 h. The antibodies used in this study were supplied by Abcam. Blots were visualized using an ECL detection reagent (Millipore), and the analysis was conducted using ImageJ version 1.52 software (as indicated in Table S3).

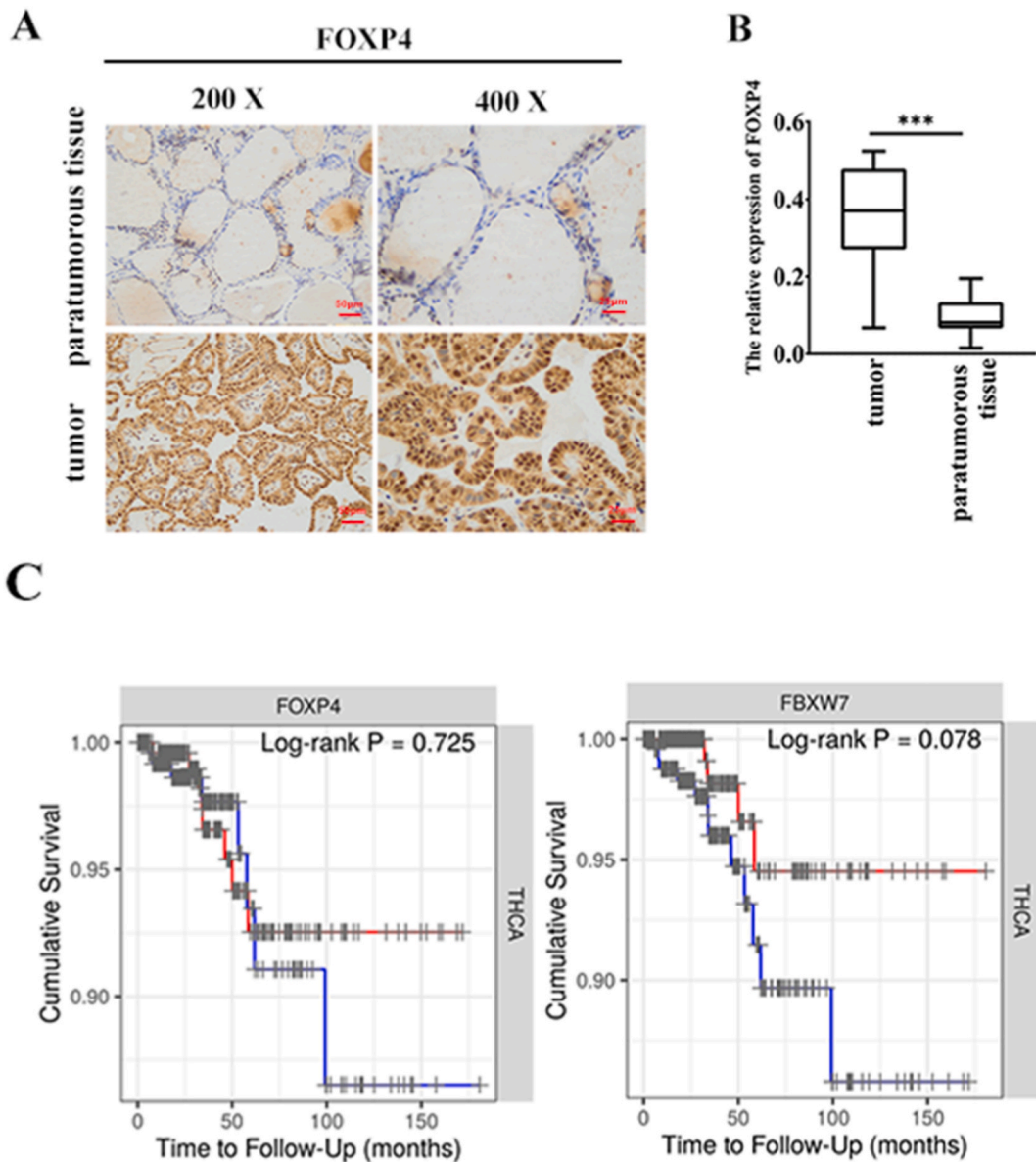


**Fig. 1. FOXP4 in thyroid tissue** (A) The levels of FOXP4 in thyroid cancer and adjacent tissues were determined by immunohistochemistry. (B) Semi-quantitative results of immunohistochemistry. (C) The relationship between the survival rate of patients with FOXP4 and FBXW7 levels was analyzed using the TIMER web server. \*\*\* $P < 0.001$ .

2.11. Chromatin immunoprecipitation (ChIP)

To investigate the association between FOXP4 and FBXW7, we utilized a chromatin immunoprecipitation (ChIP) kit from Amylet, Wuhan, China. Cells were treated with 16% methanol and lysis buffer, followed by sonication to facilitate the ChIP procedure. Following sonication, cells were incubated overnight with either anti-FOXP4 or IgG antibody. Subsequently, the protein-DNA complex was collected utilizing protein A/G beads, and DNA extraction was carried out using 5 mmol/l NaCl. The concentration of FBXW7 was then assessed through PCR analysis.

2.12. Immunofluorescence (IF)

Initially, cells from Nthy-ori 3-1, KTC-1, and TPC-1 were seeded in 6-well plates. Following fixation with 4% formaldehyde for 20 min, the cells were blocked with 0.3% Triton X-100 for 5 min and treated with 2% BSA (Merck KGaA, Germany) for 30 min. Subsequently, the cells were incubated overnight at 4 °C with the FOXP4 antibody (Thermo Fisher Scientific). Afterward, the cells were stained with FITC-labeled Goat anti-rabbit secondary antibody for 1 h. Nuclei were counterstained with DAPI for 5 min, and images

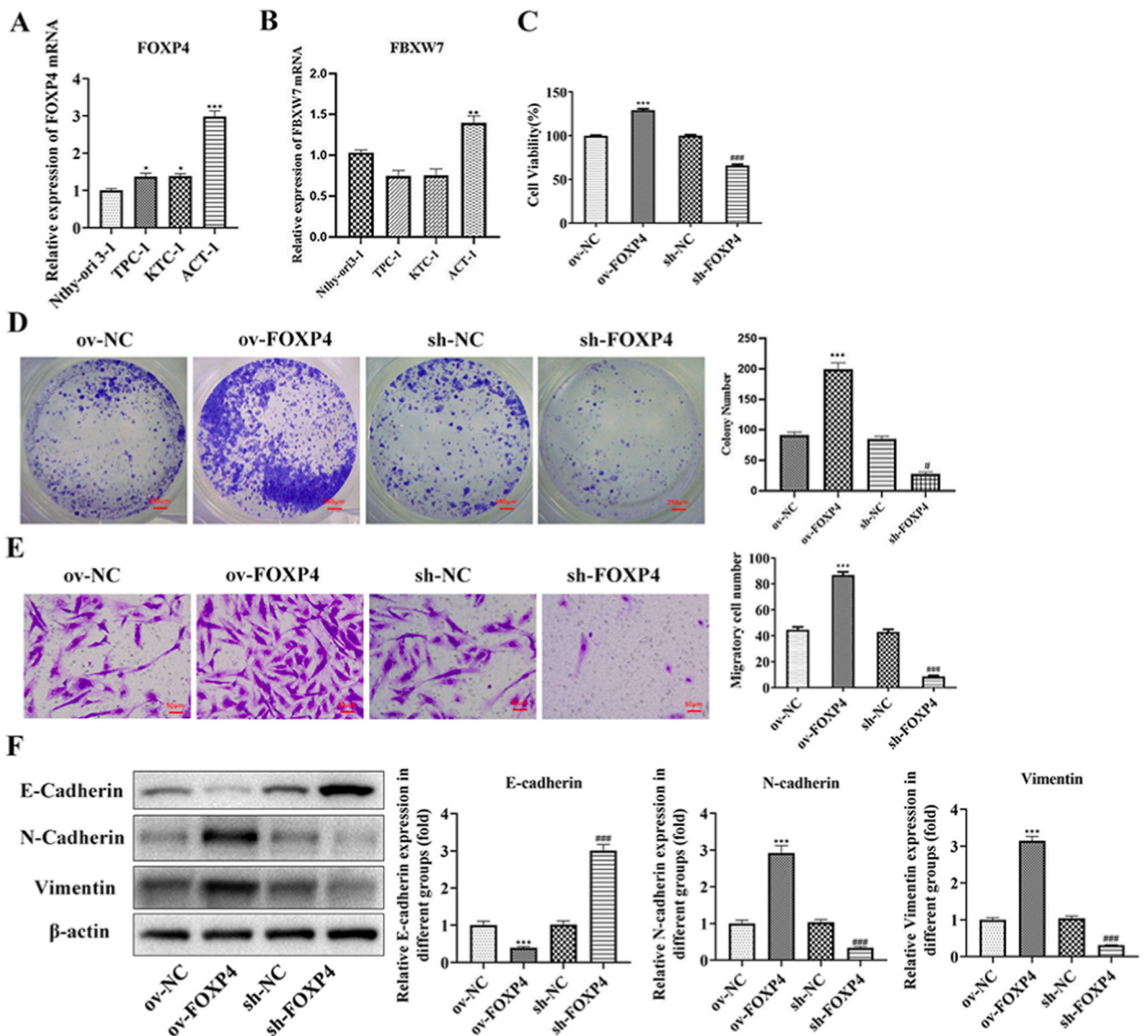


Fig. 2. FOXP4 in thyroid cancer cells (A) The levels of FOXP4 and (B) FBXW7 in thyroid cancer cells were determined by RT-qPCR. (C) The effects of FOXP4 knockdown or overexpression on cell viability and (D) colony formation ability were assessed using the CCK8 and colony formation assay. (E) Cell migration was evaluated using Transwell assay. (F) The EMT process was assessed using western blotting. \* $P < 0.05$ , \*\* $P < 0.01$ , \*\*\* $P < 0.001$  vs. Nthy-ori3-1 or ov-NC; # $P < 0.05$ , ## $P < 0.01$ , ### $P < 0.001$  vs. sh-NC.

were captured using a confocal microscope (Model: SpinSR10, Software: Cell Sens Dimension 4.2, Leica, Germany).

### 2.13. Bioinformatics and statistical analysis

All experiments were conducted independently and repeated a minimum of three times to ensure reliability. Data were analyzed using Prism 8.0 software and presented as mean  $\pm$  SD (standard deviation). Statistical comparisons among multiple groups were performed using one-way ANOVA followed by Tukey's post hoc test. Differences between two groups were assessed using Student's *t*-test. A significance level of  $P < 0.05$  was considered statistically significant.

### 2.14. Statistical analysis

Statistical analysis was carried out using SPSS 28.0 software. Normally distributed measurement data are expressed as mean  $\pm$  standard deviation. Inter-group comparisons were performed using independent sample *t*-tests or Kruskal-Wallis rank sum tests, depending on the data distribution. Counting data are presented as examples (%) to describe data distribution, and inter-group comparisons were made using chi-squared tests or Fisher's exact tests. A significance level of  $P < 0.05$  was considered statistically significant.

## 3. Results

### 3.1. Comparison of general patient information

There were no statistically significant differences observed in age, gender, multifocal occurrences, bilateral involvement, combined Hashimoto's thyroiditis (HT), tumor size, and thyroid function-related indicators among patients exhibiting differential expression of Fox4 ( $P > 0.05$ ). However, significant differences were found in lymph node metastasis and extraglandular invasion among patients with varying levels of Fox4 expression ( $P < 0.05$ ). Patients with high Fox4 expression displayed higher rates of lymph node metastasis and extraglandular invasion compared to those with low Fox4 expression (Table S4).

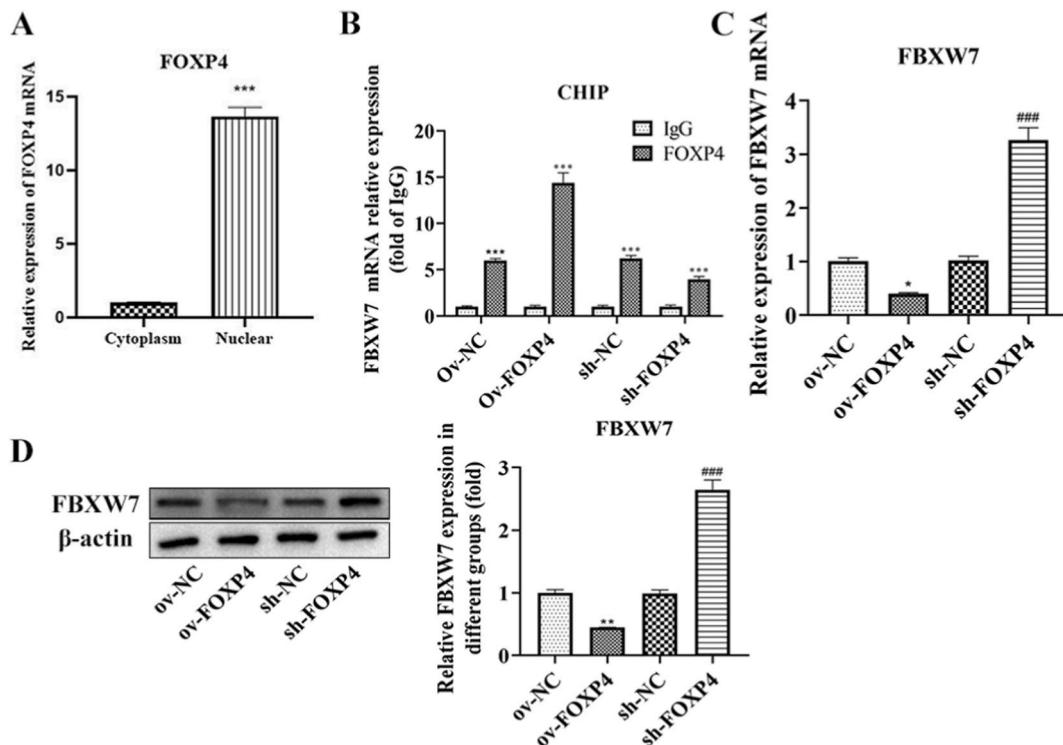


**Fig. 3. FOXP4 negatively regulates FBXW7** (A) The distribution of FOXP4 in the nucleus and nucleoplasm was determined by RT-qPCR. (B) The connection between FOXP4 and FBXW7 was verified by the ChIP assay. (C) The levels of FBXW7 in the transfected cells were examined using RT-qPCR and (D) western blotting. \* $P < 0.05$ , \*\* $P < 0.01$ , \*\*\* $P < 0.001$  vs. Cytoplasm or ov-NC; ### $P < 0.001$  vs. sh-NC.

3.2. FOXP4 and FBXW7 in thyroid tissue

Immunohistochemistry was employed to assess FOXP4 expression in TC as well as the surrounding tissues (as depicted in Fig. 1A). The quantitative box plot analysis (Fig. 1B) corroborated these findings, indicating elevated FOXP4 expression in TC tissues in comparison to the surrounding tissues. According to the analysis conducted using the TIMER web server, patients in the high-level

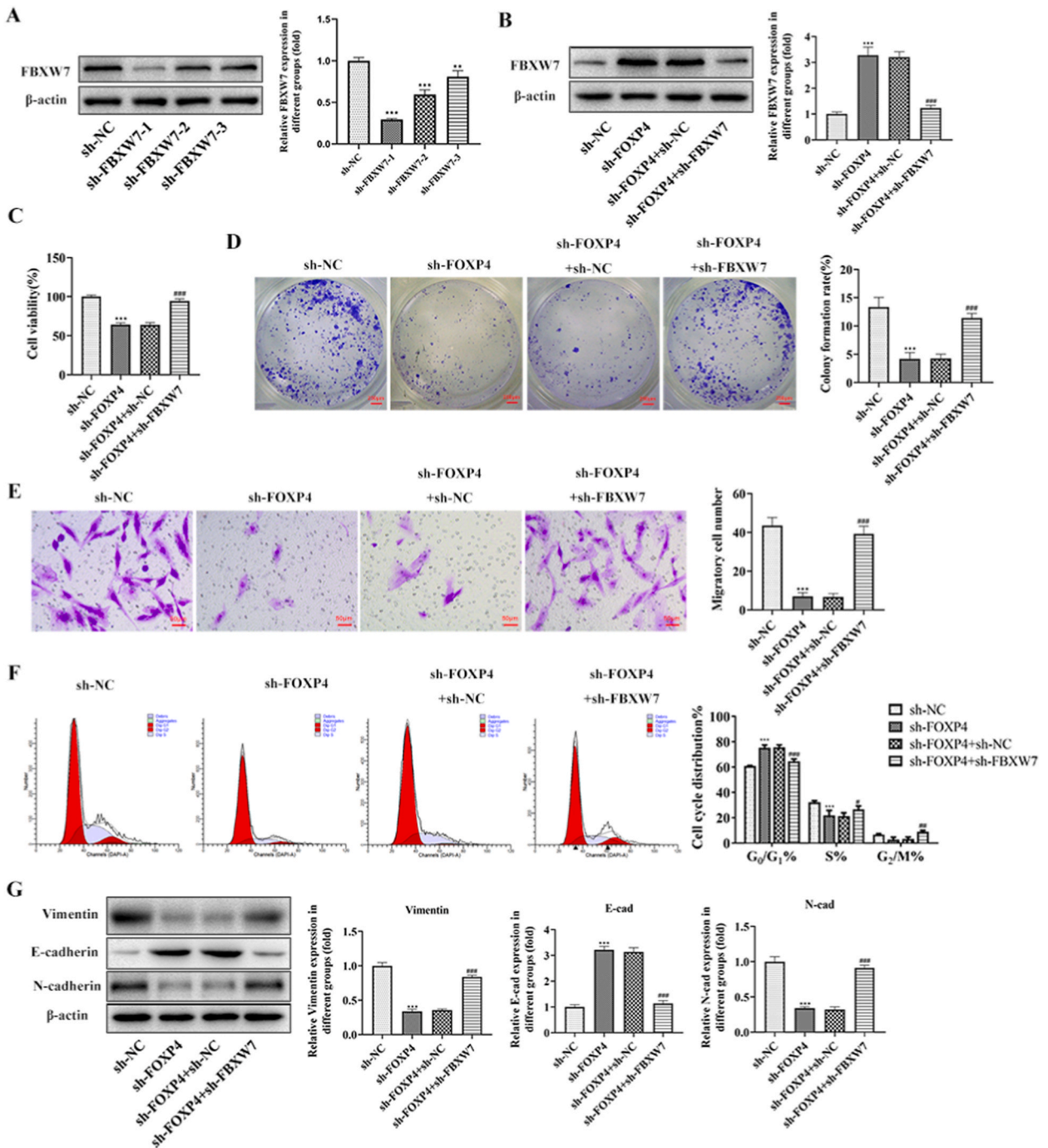


**Fig. 4.** FBXW7 affects FOXP4 functions (A) The efficacy of FBXW7 knockdown was determined by western blotting. (B) Cells were co-transfected to knock down FBXW7 along with FOXP4 knockdown, and the level of FBXW7 was determined by western blotting. (C) The impacts of FBXW7 on FOXP4 functions were assessed based on cell viability, (D) colony formation ability, (E) migration, (F) cell cycle, and (G) EMT process. \*\* $P < 0.01$ , \*\*\* $P < 0.001$  vs. sh-NC; \* $P < 0.05$ , ## $P < 0.01$ , ### $P < 0.001$  vs. sh-FOXP4 + sh-NC.

FOXP4 group exhibited a higher survival rate than those in the low-level group within the initial 3 years. In contrast, patients in the low-level group demonstrated a higher survival rate within the 3 to 6-year period; however, the difference between the two groups during this time frame was not statistically significant (Fig. 1C).

3.3. FOXP4 in TC cells

The contents of FOXP4 and FBXW7 in epithelial and cancer cells were analyzed to gain insights into their functions. It was observed that the expression of FOXP4 was higher in all three types of cancer cells. Conversely, FBXW7 expression was lower in TPC-1 and KTC-1 cells but higher in ACT-1 cells (Fig. 2A–B). Given the association of low expression with a favorable short-term prognosis, the KTC-1 cell line, characterized by low FOXP4 levels, was selected for in-depth research into the potential roles of these genes in cancers with poor prognoses. In this context, KTC-1 cells were subjected to transfection protocols to either knock down or overexpress FOXP4. Subsequently, cell viability (Fig. 2C) and colony formation ability (Fig. 2D) were assessed in the study. In comparison to the NC group,

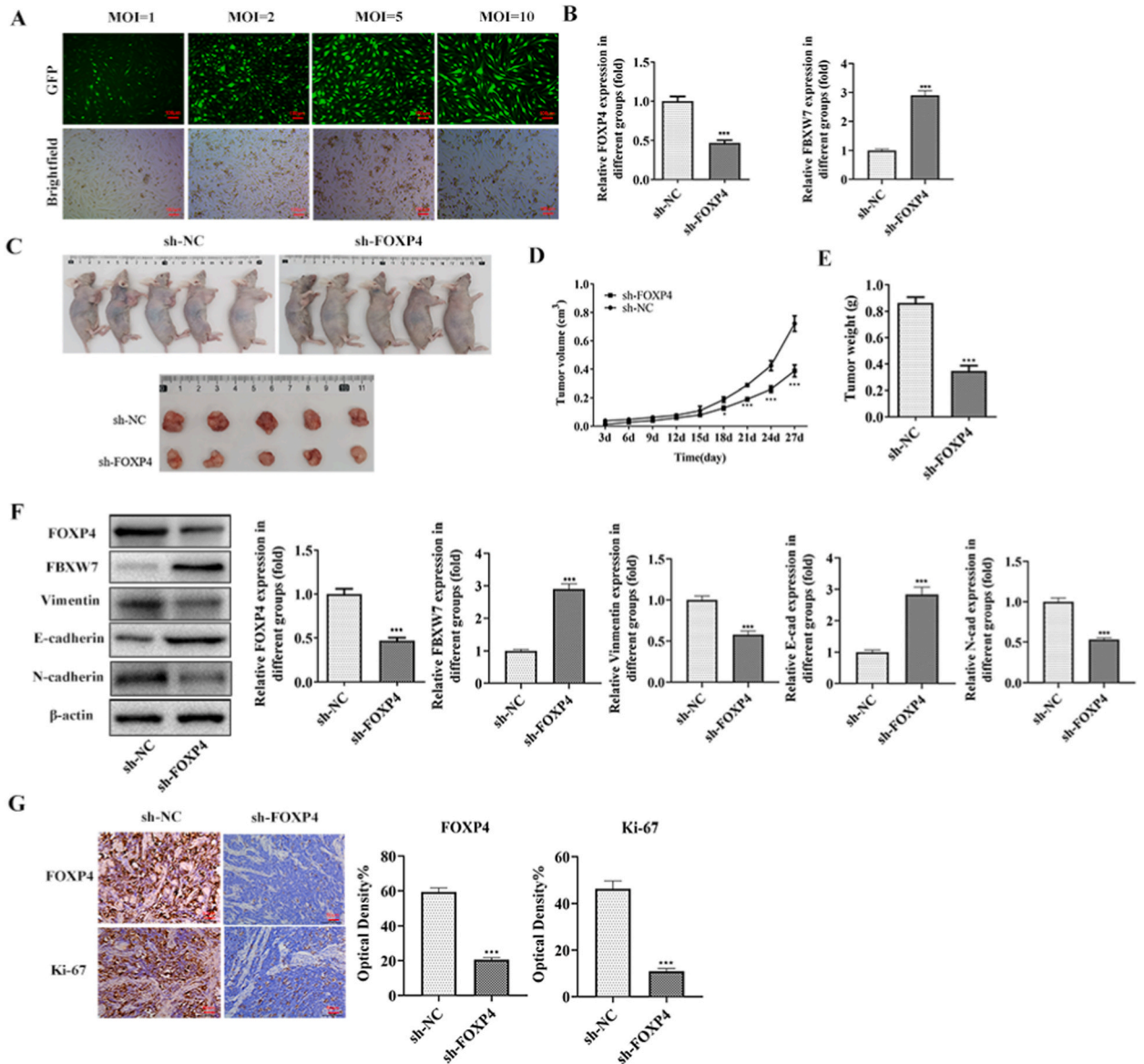


**Fig. 5. Tumor formation in nude mice** (A) Stably transfected cell lines were constructed, MOI = 5 group was used for tumor transplantation. (B) The levels of FOXP4 and FBXW7 in stably transfected KTC-1 cells were examined using western blotting. (C) Photos of mice and tumors. (D) The effects of FOXP4 knockdown on the tumor volume growth and (E) weight were recorded. (F) The expression levels of EMT-related protein in tumors were determined using western blotting. (G) The expression levels of Ki67 protein in tumors were determined using western blotting. \*\*\**P* < 0.001 vs. sh-NC.

the cell viability and colony formation potential markedly increased in the ov-FOXP4 group, and decreased in the sh-FOXP4 group. Subsequently, the cell migration ability was evaluated utilizing a Transwell assay. FOXP4 overexpression was found to induce cell migration, whereas knockdown had the opposite effect (Fig. 2E). Additionally, the impact of FOXP4 levels on EMT was assessed through western blotting. High levels of FOXP4 led to increased N-cadherin and vimentin expression while reducing E-cadherin enrichment. Conversely, decreased FOXP4 levels resulted in the opposite effect (Fig. 2F).

### 3.4. FOXP4 negatively regulates FBXW7

The RT-qPCR results revealed that FOXP4 was predominantly localized in the nucleus (Fig. 3A). ChIP experiments demonstrated the binding of FOXP4 and FBXW7, with FBXW7 levels in the precipitated complex significantly higher than IgG levels (Fig. 3B). Subsequently, RT-qPCR and western blotting were utilized to assess FBXW7 expression in the transfected cells. As illustrated in Fig. 3C–D, there exists a negative correlation between FOXP4 and FBXW7 in KTC-1 cells. Following the confirmation of effective FBXW7 knockdown, cells were co-transfected to further downregulate FBXW7 alongside FOXP4. This co-transfection led to a substantial decrease in FBXW7 expression (Fig. 4A–B). Subsequently, various cellular processes including viability, colony-forming ability, cell migration, cell cycle, and EMT were analyzed (Fig. 4C–G). In comparison to the sh-FOXP4 + sh-NC group, depleting FBXW7 enhanced cell viability, colony-forming ability, cell migration, growth, and EMT processes.

### 3.5. Tumor formation in nude mice

For tumor transplantation, a Multiplicity of Infection (MOI) of 5 group was selected based on fluorescence intensity (Fig. 5A). The stably transfected KTC-1 cells demonstrated reduced levels of FOXP4 and elevated levels of FBXW7 (Fig. 5B). The effective knockdown of FOXP4 significantly decelerated tumor volume growth, with the tumor weight also being lower than that in the sh-NC group (Fig. 5C–E). In exfoliated tumors, FOXP4 knockdown resulted in increased levels of FBXW7 and epithelial-related proteins while decreasing the levels of mesenchymal-related proteins, indicating that FOXP4 can promote EMT in vivo (Fig. 5F). Furthermore, immunohistochemical results revealed that FOXP4 knockdown led to reduced Ki67 protein enrichment, indicating decreased cell proliferation (Fig. 5G).

## 4. Discussion

Early-stage TC is generally less aggressive and offers a better prognosis after treatment. Surgical intervention currently enjoys a high success rate in these cases. However, the same cannot be said for advanced types of cancer characterized by high invasiveness and a significant metastatic potential [15]. Hence, the primary objective of thyroid cancer (TC) research is to identify the fundamental molecules and regulatory pathways governing TC invasion and metastasis [22]. In clinical practice, understanding these factors can facilitate the early diagnosis of patients with a poor prognosis, enabling prompt and effective treatment strategies [23]. This research demonstrated that elevated levels of FOXP4 in KTC-1 cells facilitated cell proliferation, migration, and the EMT. Analysis of metastatic pleural effusion in KTC-1 cells [24] revealed their enhanced migratory potential compared to cancer cells isolated from the primary lesion. The EMT process weakens and disrupts connections between epithelial cells, enhancing tumor cell motility and migration, ultimately increasing tumor cell invasiveness and the likelihood of distant metastasis [25,26].

Elevated levels of FOXP4 have been associated with clinical features of human hepatocellular carcinoma [20]. Furthermore, FOXP4 upregulation has been shown to promote breast cancer cell proliferation and invasion [19]. Although the exact role of FOXP4 in TC is not yet fully understood, a recent study proposed that a decrease in FOXP2 might influence immune cell infiltration and contribute to tumor recurrence [27]. It is crucial to acknowledge that the study mentioned above relies on bioinformatics analysis, and further experimental investigations are necessary to validate these findings.

The protein encoded by FBXW7 belongs to the F-box protein family and plays a crucial role in identifying and binding phosphorylated substrates, thereby regulating their turnover [28]. Oncogenes such as cyclin E, c-myc, c-jun, and Notch are degraded through the FBXW7-mediated ubiquitin-proteasome pathway [29]. These genes contribute to cancer cell proliferation, and their accumulation can be triggered by FBXW7 mutations and deletions. Mutations and allelic deletions of FBXW7 are frequently observed in a variety of human cancers [30–32]. Exonic mutations in FBXW7 in differentiated and poorly differentiated thyroid carcinoma [33], as well as FBXW7 deficiency in patients with follicular type TC [34] were found through genome sequencing. Nevertheless, FBXW7 is biallelic, therefore, simple loss-of-function mutations are rare [35]. The results from the cellular experiments conducted in this study support the notion that FBXW7 operates as a tumor suppressor in TC characterized by a poor prognosis. However, it is important to note that information regarding the presence of FBXW7 mutations in KTC-1 cells was not available. Moreover, the results of this study demonstrate that FOXP4 can regulate the transcription of FBXW7, leading to the dysregulation of FBXW7 expression.

It is important to acknowledge the limitations of this study, primarily due to the insufficient availability of clinical samples featuring poor prognosis for comprehensive comparison.

In summary, the findings from this study demonstrate that FOXP4 has the capacity to regulate FBXW7 transcription, leading to the disruption of FBXW7 expression. This dysregulation of FBXW7 contributes to the malignant characteristics observed in highly invasive TC cells. Targeting FOXP4 could potentially impede the growth and dissemination of cancer cells, offering a promising treatment approach for thyroid cancer types associated with a poor prognosis.

## Funding

Regional Fund Cultivation Program of National Natural Science Foundation of China (NSFC) of Guizhou Medical University (gyfynsfc-2022-54).

BeiJing Health Promotion Association Chinese Surgery Young Physician Research Project Support Project (CJBSRAF-2022).  
Science and Technology Fund of Guizhou Provincial Health Commission (No. gzwkj2021-170).

## CRediT authorship contribution statement

**Tian Zhou:** Writing – original draft, Data curation, Conceptualization. **Ning Ma:** Writing – original draft, Formal analysis, Data curation. **Yong-lin Zhang:** Writing – original draft, Investigation, Formal analysis. **Xing-hong Chen:** Writing – original draft, Software, Investigation. **Xue Luo:** Writing – original draft, Software, Resources. **Mai Zhang:** Writing – original draft, Supervision, Resources. **Qing-jun Gao:** Writing – review & editing, Writing – original draft, Software, Resources, Formal analysis. **Dai-wei Zhao:** Writing – review & editing, Writing – original draft, Project administration, Methodology, Conceptualization.

## Declaration of competing interest

The authors declare that they have no known competing financial interests or personal relationships that could have appeared to influence the work reported in this paper.

## Appendix A. Supplementary data

Supplementary data to this article can be found online at <https://doi.org/10.1016/j.heliyon.2023.e23875>.

## References

- [1] L. Alexander, N. Patel, M. Caserta, M. Robbin, Thyroid ultrasound: diffuse and nodular disease, *Radiol. Clin. North Am.* 58 (2020) 1041–1057.
- [2] T. Todsen, F. Bennedbaek, K. Kiss, L. Hegedüs, Ultrasound-guided fine-needle aspiration biopsy of thyroid nodules, *Head Neck* 43 (2021) 1009–1013.
- [3] J. Jun, S. Hwang, S. Hong, M. Suh, K. Choi, K. Jung, Association of screening by thyroid ultrasonography with mortality in thyroid cancer: a case-control study using data from two national surveys, *Thyroid* 30 (2020) 396–400.
- [4] S. Wirth, M.E. Syleouni, N. Karavasiloglou, S. Rinaldi, D. Korol, M. Wanner, S. Rohrmann, Incidence and mortality trends of thyroid cancer from 1980 to 2016, *Swiss Med. Wkly.* 151 (2021 Nov 5) w30029.
- [5] W. Cao, H. Chen, Y. Yu, N. Li, W. Chen, Changing profiles of cancer burden worldwide and in China: a secondary analysis of the global cancer statistics 2020, *Chin. Med. J. (Engl.)* 134 (2021) 783–791.
- [6] A. Prete, P. Borges de Souza, S. Censi, M. Muzza, N. Nucci, M. Sponziello, Update on fundamental mechanisms of thyroid cancer, *Front. Endocrinol.* 11 (2020) 102.
- [7] T. Wang, J. Sosa, Thyroid surgery for differentiated thyroid cancer - recent advances and future directions, *Nat. Rev. Endocrinol.* 14 (2018) 670–683.
- [8] G. Grani, L. Lamartina, C. Durante, S. Filetti, D. Cooper, Follicular thyroid cancer and Hürthle cell carcinoma: challenges in diagnosis, treatment, and clinical management, *Lancet Diabetes Endocrinol.* 6 (2018) 500–514.
- [9] T. Ibrahimspic, R. Ghossein, J. Shah, I. Ganly, Poorly differentiated carcinoma of the thyroid gland: current status and future prospects, *Thyroid* 29 (2019) 311–321.
- [10] M. Tesselaaar, J. Smit, J. Nagarajah, R. Netea-Maier, T. Plantinga, Pathological processes and therapeutic advances in radioiodide refractory thyroid cancer, *J. Mol. Endocrinol.* 59 (2017) R141–r154.
- [11] G.L. Francis, S.G. Waguespack, A.J. Bauer, P. Angelos, S. Benvenga, J.M. Cerutti, C.A. Dinauer, J. Hamilton, I.D. Hay, M. Luster, M.T. Parisi, M. Rachmiel, G. B. Thompson, S. Yamashita, American thyroid association guidelines task force. Management guidelines for children with thyroid nodules and differentiated thyroid cancer, *Thyroid* 25 (7) (2015 Jul) 716–759.
- [12] A. McDow, S. Pitt, Extent of surgery for low-risk differentiated thyroid cancer, *Surg. Clin.* 99 (2019) 599–610.
- [13] W. Zhao, L. You, X. Hou, S. Chen, X. Ren, G. Chen, Y. Zhao, The effect of prophylactic central neck dissection on locoregional recurrence in papillary thyroid cancer after total thyroidectomy: a systematic review and meta-analysis : pCND for the locoregional recurrence of papillary thyroid cancer, *Ann. Surg. Oncol.* 24 (8) (2017 Aug) 2189–2198.
- [14] K. Gršić, B. Bumber, R. Curić Radivojević, D. Leović, Prophylactic central neck dissection in well-differentiated thyroid cancer, *Acta Clin. Croat.* 59 (2020) 87–95.
- [15] M. Cabanillas, M. Ryder, C. Jimenez, Targeted therapy for advanced thyroid cancer: kinase inhibitors and beyond, *Endocr. Rev.* 40 (2019) 1573–1604.
- [16] Q.Z. Long, Y.F. Du, X.Y. Ding, X. Li, W.B. Song, Y. Yang, P. Zhang, J.P. Zhou, X.G. Liu, Replication and fine mapping for association of the C2orf43, FOXP4, GPRC6A and RFX6 genes with prostate cancer in the Chinese population, *PLoS One* 7 (5) (2012) e37866.
- [17] A.L. Chokas, C.M. Trivedi, M.M. Lu, P.W. Tucker, S. Li, J.A. Epstein, E.E. Morrissey, Foxp1/2/4-NuRD interactions regulate gene expression and epithelial injury response in the lung via regulation of interleukin-6, *J. Biol. Chem.* 285 (17) (2010 Apr 23) 13304–13313.
- [18] P. Xue, S. Huang, X. Han, C. Zhang, L. Yang, W. Xiao, J. Fu, H. Li, Y. Zhou, Exosomal miR-101-3p and miR-423-5p inhibit medulloblastoma tumorigenesis through targeting FOXP4 and EZH2, *Cell Death Differ.* 29 (1) (2022 Jan) 82–95.
- [19] T. Ma, J. Zhang, Upregulation of FOXP4 in breast cancer promotes migration and invasion through facilitating EMT, *Cancer Manag. Res.* 11 (2019) 2783–2793.
- [20] G. Zhang, G. Zhang, Upregulation of FoxP4 in HCC promotes migration and invasion through regulation of EMT, *Oncol. Lett.* 17 (2019) 3944–3951.
- [21] J. Shi, J. Wang, H. Cheng, S. Liu, X. Hao, L. Lan, G. Wu, M. Liu, Y. Zhao, FOXP4 promotes laryngeal squamous cell carcinoma progression through directly targeting LEF-1, *Mol. Med. Rep.* 24 (6) (2021 Dec) 831.
- [22] C. Zafon, J. Gil, B. Pérez-González, M. Jordà, DNA methylation in thyroid cancer, *Endocr. Relat. Cancer* 26 (2019) R415–r439.
- [23] M. Schlumberger, S. Leboulleux, Current practice in patients with differentiated thyroid cancer, *Nat. Rev. Endocrinol.* 17 (2021) 176–188.
- [24] J. Kurebayashi, K. Tanaka, T. Otsuki, T. Moriya, H. Kunisue, M. Uno, H. Sonoo, All-trans-retinoic acid modulates expression levels of thyroglobulin and cytokines in a new human poorly differentiated papillary thyroid carcinoma cell line, KTC-1, *J. Clin. Endocrinol. Metab.* 85 (8) (2000 Aug) 2889–2896.
- [25] G. Babaei, S. Aziz, N. Jaghi, EMT, cancer stem cells and autophagy: the three main axes of metastasis, *Biomed. Pharmacother.* 133 (2021) 110909.

- [26] T. Holm, S. Yeo, K. Turner, J. Guan, Targeting autophagy in thyroid cancer: EMT, apoptosis, and cancer stem cells, *Front. Cell Dev. Biol.* 10 (2022) 821855.
- [27] L. Xu, Z. Yang, Q. Zhao, H. Feng, J. Kuang, Z. Liu, L. Chen, L. Zhan, J. Yan, W. Cai, W. Qiu, Effect of FOXP2 transcription factor on immune infiltration of thyroid cancer and its potential clinical value, *Front. Immunol.* 13 (2022 Sep 20) 982812.
- [28] J. Fan, M. Bellon, M. Ju, L. Zhao, M. Wei, L. Fu, C. Nicot, Clinical significance of FBXW7 loss of function in human cancers, *Mol. Cancer* 21 (1) (2022 Mar 26) 87.
- [29] C. Yeh, M. Bellon, C. Nicot, FBXW7: a critical tumor suppressor of human cancers, *Mol. Cancer* 17 (2018) 115.
- [30] K. Yumimoto, K. Nakayama, Recent insight into the role of FBXW7 as a tumor suppressor, *Semin. Cancer Biol.* 67 (2020) 1–15.
- [31] K. Korphaisarn, V.K. Morris, M.J. Overman, D.R. Fogelman, B.K. Kee, K.P.S. Raghav, S. Manuel, I. Shureiqi, R.A. Wolff, C. Eng, D. Menter, S.R. Hamilton, S. Kopetz, A. Dasari, FBXW7 missense mutation: a novel negative prognostic factor in metastatic colorectal adenocarcinoma, *Oncotarget* 8 (24) (2017 Jun 13) 39268–39279.
- [32] M. Urlick, E. Yu, D. Bell, High-risk endometrial cancer proteomic profiling reveals that FBXW7 mutation alters L1CAM and TGM2 protein levels, *Cancer* 127 (2021) 2905–2915.
- [33] T. Gerber, A. Schad, N. Hartmann, E. Springer, U. Zechner, T. Musholt, Targeted next-generation sequencing of cancer genes in poorly differentiated thyroid cancer, *Endocr. Connect* 7 (2018) 47–55.
- [34] M. Borowczyk, E. Szczepanek-Parulska, S. Dębicki, B. Budny, F.A. Verburg, D. Filipowicz, B. Więckowska, M. Janicka-Jedyńska, L. Gil, K. Ziemnicka, M. Ruchała, Differences in mutational profile between follicular thyroid carcinoma and follicular thyroid adenoma identified using next generation sequencing, *Int. J. Mol. Sci.* 20 (13) (2019 Jun 26) 3126.
- [35] H. Davis, I. Tomlinson, CDC4/FBXW7 and the 'just enough' model of tumourigenesis, *J. Pathol.* 227 (2012) 131–135.